

On robustness against evacuees' unexpected movement in automatic evacuation guiding

Jun Kawahara^a, Takanori Hara^b, Masahiro Sasabe^b

^aGraduate School of Informatics, Kyoto University, Yoshida Honmachi, Sakyo-ku, 6068501, Kyoto, Japan

^bGraduate School of Science and Technology, Nara Institute of Science and Technology, Takayama 8916-5, Ikoma, 6300192, Nara, Japan

Abstract

The automatic evacuation guiding using mobile devices is a promising disaster-response approach for large-scale disasters. When a disaster occurs, each mobile device **recommends** a route **to a refuge** and automatically estimates the state of road segments by **comparing** the recommended route and **observed trajectory**. The estimated information is shared among devices using available communication technologies. This scheme assumes that each evacuee follows the recommended route but it might not be satisfied when an evacuee behaves as an outlier taking unexpected movement, **which** will disturb the normal evacuation. This paper analyzes the effects of outliers and reveals the following characteristics through simulations: **T**he number of passable road segments misestimated as impassable increases with outliers; Many of them, however, can be corrected by passable estimation from other outliers; The remaining misestimation **increases** the evacuation completion time of **26.5% of** normal evacuees **by more than 100 seconds**. Since the speedy and accurate outlier detection **is** difficult in the severe communication environments, this paper alternatively proposes a mechanism that delays to judge a road segment as impassable until gathering the corresponding impassable estimation from M devices. The simulation results show that $M = 2$ achieves a balance between the speediness and safety in evacuation guiding.

Keywords: Automatic evacuation guiding, Robustness against evacuees' unexpected movement, Misestimation of road state, Device-to-device communications

1. Introduction

With the proliferation of mobile devices such as smartphones, there have been studied disaster-response approaches (e.g., information gathering and evacuation guiding) supported by them for large-scale disasters such as the Nankai Trough Earthquake [1, 2, 3]. In particular, **our research group has** proposed an automatic evacuation guiding scheme using mobile devices under a large-scale disaster **to liberate evacuees from manually registering the road-state information to their devices** [3].

Email addresses: jkawahara@i.kyoto-u.ac.jp (Jun Kawahara), hara.takanori@is.naist.jp (Takanori Hara), m-sasabe@ieee.org (Masahiro Sasabe)

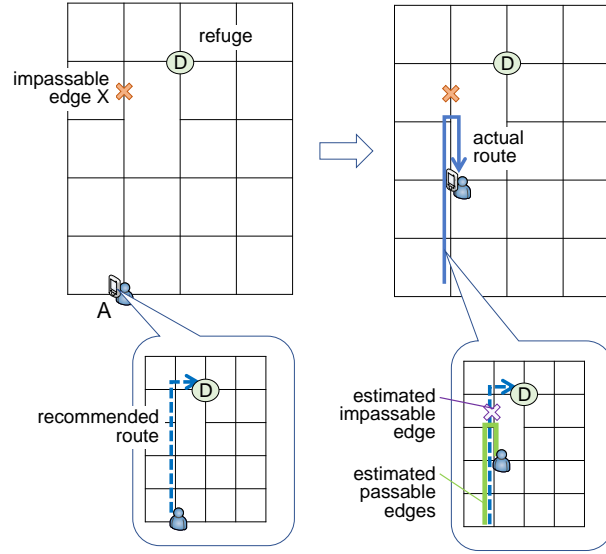


Figure 1: An example flow of the automatic evacuation guiding scheme [3]. The grid represents a road network, which consists of passable edges except one impassable edge X. In the left figure, an evacuee A tries to move to a refuge D along with the recommended route given by A’s device. Then, in the right figure, the evacuee A encounters the impassable edge and takes a detour.

In the scheme, an evacuee pre-installs the proposed application into his/her mobile device (hereinafter referred to as *device*). When a disaster occurs, the device recommends a route from the current location, which is measured by the Global Positioning System (GPS), to a refuge and the evacuee is expected to follow the recommended route (the left side in Figure 1). If the evacuee encounters an impassable road segment (hereinafter referred to as *edge*) on the recommended route due to debris from the disaster, the evacuee is expected to divert the route at his/her own discretion (the right side in Figure 1). At the same time, the application can detect the deviation from its recommended route by checking the difference with his/her movement (i.e., **observed** trajectory) composed of his/her positions observed by GPS. As a result, it can automatically estimate the state of the edge causing the difference as impassable.

The information on edges estimated as impassable is shared among other devices via available communication technologies such as communication infrastructures (e.g., cellular networks and wireless LANs) and/or Delay Tolerant Networks (DTNs) [4]. DTN enables the end-to-end communications by using the device-to-device (D2D) communications (e.g., Bluetooth and Wi-Fi Direct), where two devices in their transmission range directly communicate with each other. Consequently, the devices with the subsequent evacuees can improve their evacuation by calculating their recommended routes without the edges estimated as impassable.

In the automatic evacuation guiding scheme, the estimation accuracy of impassable edges has a significant impact on evacuation support. In the previous work [3], Komatsu et al. assumed that each evacuee

follows his/her recommended route provided by his/her application. This assumption, however, might not (temporarily) be satisfied. For example, some evacuees may move to their own destinations (e.g., home, office, or (pre)schools), which differ from the designated refuges. More complex movement may also occur, e.g., moving to the refuges after visiting one or more other facilities, but it is difficult to consider all possible patterns of such unexpected movement. In this paper, as a first step, we focus on the simple unexpected movement pattern (i.e., moving to the different destinations from the designated refuges) and refer to it as *unexpected evacuation movement*. We also refer to evacuees taking such unexpected evacuation movement as *outliers* and those following the recommended routes as *normal evacuees* (or *evacuees* simply). Please note that the proposed applications of the outliers' devices also work in the background because they cannot recognize the type (normal or outlier) of their owners. As in the discussion about the unexpected movement, there seem to be various patterns in whether/how the outliers use the information presented by their devices (i.e., passable/impassable estimation of edges). In this paper, we simply assume that the outliers, which try to move their own destinations, do not use the recommended routes as well as the estimated information given by their devices.

Unexpected evacuation movement may cause misestimation of passable edges as impassable. Figure 2 shows the process of misestimation of passable edges as impassable by such unexpected evacuation movement and its negative impact on the normal evacuation movement. Subsequent evacuees receiving misestimated information from earlier evacuees may be forced to conduct unnecessary detours or cannot find any recommended routes in the worst case.

On the other hand, the presence of outliers may have a positive impact on the normal evacuation movement in terms of finding and sharing more passable edges. In the previous work [5], Hara et al. extended the automatic evacuation guiding scheme [3] by adding a mechanism to share not only impassable edges but also passable ones among devices. Each device can estimate the edges included in the *observed* trajectory as passable. The information on passable edges can improve the safety of recommended routes in the route selection. Furthermore, the misestimation of passable edge(s) as impassable by an outlier can be corrected by passable information from other outliers as shown in Figure 3. Note that we assume that passable edges can be estimated *more accurately* than impassable ones. (The validity of this assumption will be discussed in Section 3.) This illustration presents the possibility that the estimation and sharing of passable edges by outliers may improve the evacuation movement of the subsequent normal evacuees. *The above* discussion indicates that the impact of unexpected evacuation movement is not necessarily simple.

The contributions of the paper are as follows:

- *To clarify the complex situation described above*, we quantitatively analyze the impact of unexpected evacuation movement on the automatic evacuation guiding scheme *through simulations (Section 4)*. *To the best of our knowledge, this is the first work on tackling the misestimation problem specific to*

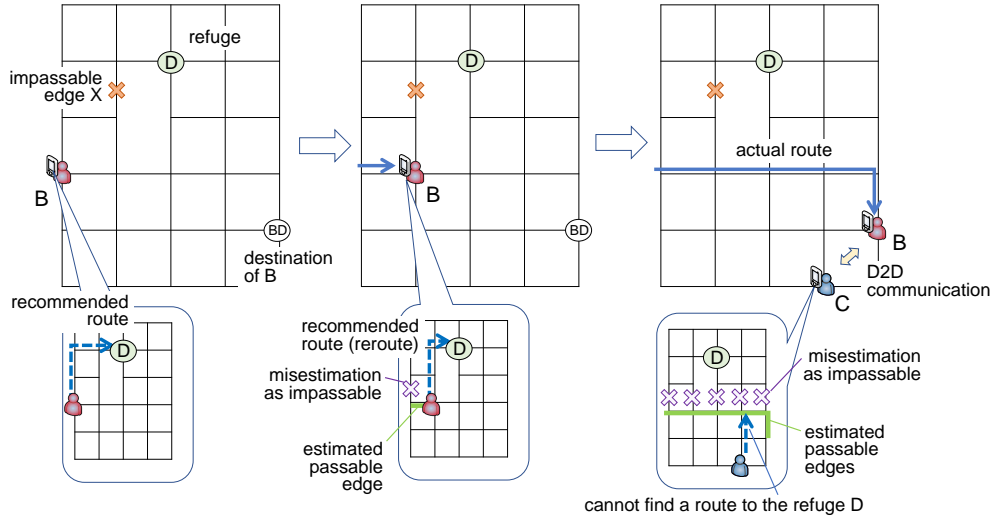


Figure 2: The process of misestimation of passable edges as impassable and its negative impact on the normal evacuation movement. In the left figure, the outlier B’s device presents the recommended route to the refuge D. Next, in the middle figure, the outlier B starts moving to his/her own destination (BD), which causes the misestimation of the passable edge as impassable. In the right figure, such misestimation is repeated with his/her movement and shared with the normal evacuee C’s device through a D2D communication, which prevents C’s device from finding the recommended route to the refuge D.

the automatic evacuation guiding.

- To improve the robustness against the misestimation of passable edges as impassable, we propose a receiver-side mechanism that delays the decision of an edge as impassable until gathering the corresponding impassable estimation from at least $M \geq 2$ devices (Section 5.1).
- We show the effectiveness of the proposed method by simulations. We investigate the appropriate value of M and show that $M = 2$ achieves a balance between the speediness and safety in evacuation guiding, regardless of the number of evacuees (Section 5.2).

Someone might wonder why we do not try to detect the unexpected evacuation movement itself and prevent the spread of misestimated information at the sender side. This is because of the difficulty in speedy and accurate detection under the evacuation situations where each device requires much time to acquire a sufficient amount of information for the detection (e.g., its owner’s trajectory and leaving patterns from the recommended route). If the detection requires information from other devices, the severe communication environments will also delay the detection.

The organization of this paper is as follows. Section 2 describes related work on evacuation support schemes. We give the details of the existing automatic evacuation guiding scheme in Section 3. Section 4 discusses how unexpected evacuation movement affects the evacuation movement of normal evacuees through the simulation results. In Section 5, we propose a method to improve the robustness against the misestima-

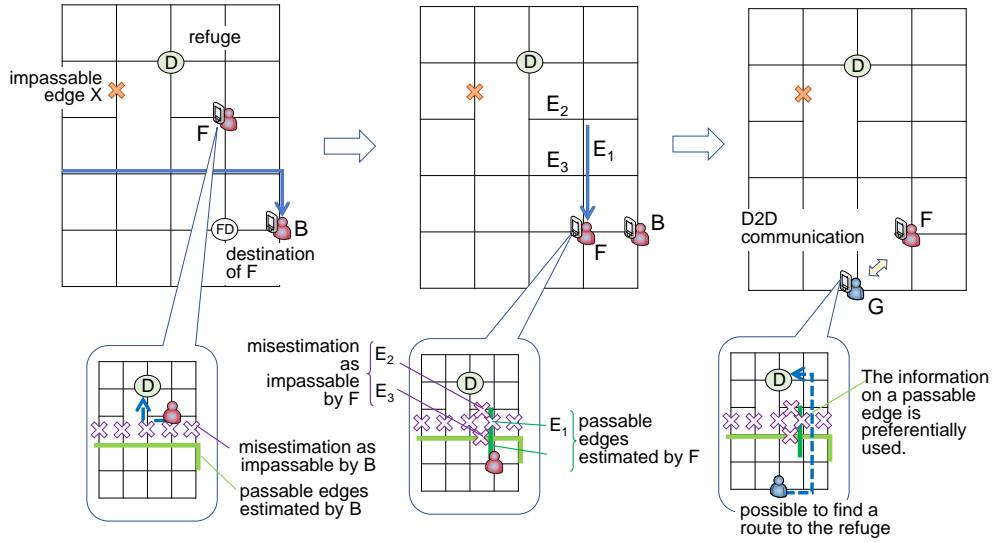


Figure 3: An example process where the misestimation of passable edges as impassable by an outlier is corrected by other outliers. The left figure shows the same situation in the right of Figure 2 except for the existence of an outlier F, where F’s device has the same information of the outlier B’s device. Since the outlier F does not use the information from the device, he/she can move to his/her own destination (FD) even under the impassable misestimation for the passable edge E_1 . In addition, this movement newly gives the correct estimation to the passable edge E_1 . Finally, in the right figure, the normal evacuee G’s device receiving the information from the outlier F’s device can find the recommended route to the refuge D.

tion and evaluate its effectiveness through the simulation results. We summarize and discuss future work in Section 6.

2. Related work

When a large-scale disaster occurs, the communication infrastructure may become unavailable due to damage to communication facilities and/or links. There are many studies on evacuation assistance to realize information sharing and/or evacuation guiding by utilizing mobile devices owned by evacuees even under such severe disaster environments.

Iizuka et al. proposed an evacuation assist system that forms an ad-hoc network among mobile devices and calculates evacuation routes to avoid congestion based on the location information of evacuees [1]. Fujihara and Miwa proposed an evacuation guiding mechanism using a DTN [2]. In this mechanism, when evacuees discover impassable edges, they manually record the information on their own mobile devices and then share it with other mobile devices through D2D communications. Nishiyama et al. clarified the system requirements applicable to many different multi-hop D2D communications under a large-scale disaster [6]. Otomo et al. built a mobile-cloud computing environment for collecting information under a disaster using a DTN [7]. Misumi et al. proposed a system to reduce the power consumption of evacuees’ mobile devices

by placing devices, called information boxes, at multiple locations, to facilitate D2D communications in an evacuation guiding system [8].

To achieve both speedy and safe evacuation, it is important to calculate an appropriate evacuation route according to the state of the road network (e.g., congestion level and road blockage risk) and the corresponding evacuee's attributes (e.g., age and sex). From the viewpoint of congestion mitigation, besides the aforementioned work [1], Kasai et al. proposed a congestion-aware evacuation route calculation method by estimating the congestion-level of each road segment based on the information collected through a DTN [9]. From the viewpoint of safe evacuation, Hara et al. proposed the risk-aware route selection, which enumerates the K -shortest route candidates and then selects the route with the maximum reachability, which is derived from road blockage probabilities, from the candidates [5]. Misumi and Kamiyama proposed an evacuation route recommendation based on the attributes of evacuees [10].

The detection of unexpected movement can be regarded as a kind of outlier (anomalous) trajectory detection. The outlier detection has been studied actively [11] and applied to various types of trajectories: hurricane tracks [12], animal movement [13], traffic flow [14, 15, 16], crowd flow [17], and so on. The outlier detection can be categorized into several methods, e.g., distance-based, density-based, clustering-based, and classification-based. The distance-based methods were first proposed by Knorr et al. [18], where the outlier trajectory is defined as a trajectory that is more than a certain distance away from other normal ones. The density-based methods were first proposed by Breunig et al. [19], where the outlier trajectory is defined as a trajectory with lower density than normal ones. The clustering-based methods [20] and classification-based methods [21] try to detect outlier trajectories by grouping similar trajectories.

These outlier detection methods commonly try to extract some features (e.g., distance, density, or similarity) to distinguish outlier trajectories from normal ones by learning from a large number of trajectories collected. **The trajectory collection, however, will delay the outlier detection and such delay tends to become large especially when the communication infrastructure is temporarily unavailable. Therefore, the outlier detection in the evacuation situations tends to be more challenging because it requires speedy and accurate estimation even under a limited number of trajectories. To the best of our knowledge, there is no appropriate outlier detection method that works under such severe situations.**

3. Existing automatic evacuation guiding scheme

In this section, we describe the details of the existing automatic evacuation guiding scheme [3] and its extension [5]. **The notation used throughout the paper is shown in Table 1.** We model the road network in the target region as an undirected graph $G = (\mathcal{V}, \mathcal{E}, f, g)$. \mathcal{V} is the set of vertices, each of which represents an intersection or a dead-end of a road segment. \mathcal{E} is the set of edges, each of which represents a road segment. $f : \mathcal{E} \rightarrow \mathbb{I}$ is a function that provides each edge $e \in \mathcal{E}$ with the road blockage probability p_e

Table 1: Notation. The symbols e, n , and t represent an edge, a device, and time, respectively. “ $kind = \text{block}$ ” (resp. “ $kind = \text{pass}$ ”) corresponds to impassable (resp. passable). $state \in \{\text{FPNB, FPLB, FBNP, FBLP}\}$.

Symbol	Description	Symbol	Description
G	Undirected graph representing a road network	T_{\max}	Simulation time
$\mathcal{V}, \mathcal{E}, \mathcal{C}$	Set of vertices, edges, and refuges	$T_{\text{server}}^{\text{kind}}(e, n)$	Time when an (im)passable pair (e, n) is stored into $\mathcal{S}_{\text{server}}^{\text{block}}$
p_e	Probability of e being blocked	$\mathcal{E}^{\text{kind}}$	Set of (im)passable edges
d_e	Distance of e	$\hat{\mathcal{E}}_n^{\text{kind}}$	Set of (im)passable edges recognized by n
\mathcal{N}	Set of devices	$\hat{\mathcal{E}}_{\text{server}}^{\text{kind}}$	Set of (im)passable edges recognized by the server
$\mathcal{N}^{\text{normal}}$	Set of devices owned by normal evacuees	$\hat{\mathcal{E}}_{\text{evac}, n}^{\text{block}}$	Set of impassable edges recognized by the evacuee with n
$\mathcal{N}^{\text{outlier}}$	Set of devices owned by outliers	$\mathcal{E}_{\text{evac}}^{\text{pass}}$	Set of actually passable edges that have been included in the recommended routes of the normal evacuees
N	Number of evacuees	$\hat{\mathcal{E}}_{\text{server}}^{\text{state}}$	Set of edges with estimated state $state$ recognized by the server
N^{normal}	Number of normal evacuees	$\mathcal{S}_n^{\text{kind}}$	Set of (im)passable pairs recognized by n
N^{outlier}	Number of outliers	$\mathcal{S}_{\text{server}}^{\text{kind}}$	Set of (im)passable pairs recognized by the server
\hat{r}_n	Route recommended by n		
r_n	Trajectory observed by n		
Δ_n	Difference of the evacuation completion time of n in Section 4.2.5		
I_{GPS}	Measurement interval using GPS		
M	Parameter that the proposed method uses		

($0 \leq p_e \leq 1$) [22], where \mathbb{I} is a real number space in range $[0, 1]$. Here, the road blockage probability p_e represents the estimated probability that each edge e would be blocked due to the collapse of buildings along the edge when an earthquake occurs [22]. Similarly, $g : \mathcal{E} \rightarrow \mathbb{R}^+$ is a function that provides each edge $e \in \mathcal{E}$ with its distance d_e , where \mathbb{R}^+ is a positive real space. The set of refuges is given by $\mathcal{C} = \{c_1, \dots, c_C\}$ ($c_i \in \mathcal{V}$, $i = 1, \dots, C$, $C = |\mathcal{C}|$), where $|\mathcal{S}|$ is the number of elements in a set \mathcal{S} . In this paper, we assume that each evacuee tries to move to the closest refuge during the evacuation. Note that the refuge selection scheme could be replaced with others, e.g., the capacitated refuge selection scheme [23].

There are $N > 0$ evacuees on the road network, each of whom owns one mobile device like a smart phone. The set of devices is denoted by $\mathcal{N} = \{1, \dots, N\}$. We assume that each evacuee pre-installs our evacuation guiding application with the map information (i.e., the graph G and the set \mathcal{C} of refuges) to the device before a disaster occurs. The application in each device can periodically measure and record its own location per $I_{\text{GPS}} > 0$ interval using a GPS sensor.

In what follows, we describe the flow of the automatic evacuation guiding scheme from the viewpoint of an evacuee who owns the device $n \in \mathcal{N}$. After a disaster occurs, some edges (i.e., road segments) on the road network would be impassable due to the collapse of buildings along them. As a result, the *state of each edge*

$e \in \mathcal{E}$ can be *passable* or *impassable*. Let $\mathcal{E}^{\text{block}}$ denote the set of impassable edges and $\mathcal{E}^{\text{pass}} = \mathcal{E} \setminus \mathcal{E}^{\text{block}}$ be the set of passable ones. All evacuees and devices do not have any information on $\mathcal{E}^{\text{block}}$ and $\mathcal{E}^{\text{pass}}$ at the start of the evacuation, and evacuees must reach one of the refuges only by going through passable edges $e \in \mathcal{E}^{\text{pass}}$. When a disaster occurs, the proposed application of the device $n \in \mathcal{N}$ starts, searches for the nearest refuge $c \in \mathcal{C}$ from the current location s obtained by GPS positioning, and calculates a recommended route \hat{r}_n to the refuge c using a route selection algorithm (the left side in Figure 1). The recommended route \hat{r}_n , which is represented as $\hat{r}_n = (s, e_1, v_1, e_2, v_2, \dots, v_{k-1}, e_k, c)$, starts from the initial location s to the refuge c via k edges $e_i \in \mathcal{E}$ ($i = 1, \dots, k$) and $k-1$ vertices $v_i \in \mathcal{V}$ ($i = 1, \dots, k-1$), where $e_i = \{v_{i-1}, v_i\}$ ($i = 1, \dots, k$) and v_0 (resp. v_k) corresponds to s (resp. c). The details of the route calculation algorithm are described in the next paragraphs. The evacuee with the device n is expected to move to the refuge c following the recommended route \hat{r}_n .

Next, we describe how the device n estimates the state of each edge $e \in \mathcal{E}$. The application of the device n periodically measures its locations (i.e., coordinates) using GPS per interval I_{GPS} and assigns it to the corresponding edge on the road network using the existing map-matching technique [24, 25]. Note that we assume that the GPS positioning error is negligible as in the previous work [3, 5]. If the estimated edge is on the recommended route \hat{r}_n , we believe that the evacuee with the device n keeps following the recommended route. Suppose a situation where the evacuee with the device n encounters an impassable edge $e_h \in \mathcal{E}^{\text{block}}$ ($2 \leq h \leq k$) on the recommended route \hat{r}_n , takes a detour at his/her own discretion, deviates from the recommended route, and is at a location s' . In this case, the application of the device n detects that the edge e' , which is obtained by map-matching with the location s' , is not included in the recommended route \hat{r}_n . At this moment, **the device n also observes its owner's trajectory** as $r_n = (s, e_1, v_1, e_2, v_2, \dots, v_{h-2}, e_{h-1}, v_{h-1}, e', s')$. By comparing the elements of \hat{r}_n and r_n from beginning to end, we observe that e_h in \hat{r}_n and e' in r_n are the first different edges among them. Therefore, the device n estimates e_h as impassable and adds it to $\hat{\mathcal{E}}_n^{\text{block}}$, which is the set of impassable edges recognized by the device n . (We add a hat to each symbol used for information estimated by devices to distinguish estimated values from true ones throughout the manuscript.) If the application of the device n detects that the edge $e \in \hat{\mathcal{E}}_n^{\text{block}}$ with impassable estimation is included in the recommended route \hat{r}_n , it newly calculates a recommended route from the current location s' to the nearest refuge $c' \in \mathcal{C}$, and the evacuee with the device n is expected to follow the newly recommended route. This process is repeated until the evacuee with the device n reaches the refuge.

In the extended version of the automatic evacuation guiding scheme [5], the application of the device n also estimates the information on passable edges in the similar manner. Suppose that the current location s'' of the evacuee with the device n obtained by GPS positioning is assigned to the corresponding edge e_ℓ ($1 \leq \ell \leq k$) by map-matching and e_ℓ is included in the recommended route \hat{r}_n , which is defined in the previous paragraphs. In this case, the path taken by the evacuee can be represented as

$r_n = (p, e_1, v_1, e_2, v_2, \dots, v_{\ell-1}, e_\ell, s'')$. The edges e_1, \dots, e_ℓ are estimated as passable and added to $\hat{\mathcal{E}}_n^{\text{pass}}$, which is the set of passable edges recognized by the device n (the right side in Figure 1). This process is performed at each interval I_{GPS} .

By sharing such edge states among evacuees, the knowledge acquired by earlier evacuees would help the evacuation of subsequent evacuees. Each device $n \in \mathcal{N}$ shares the information on impassable and passable edges with other devices $n' \in \mathcal{N}$ ($n \neq n'$) and edge/cloud server(s) (we simply call the server) on the Internet through the available communication techniques. Let $\hat{\mathcal{E}}_{\text{server}}^{\text{block}}$ and $\hat{\mathcal{E}}_{\text{server}}^{\text{pass}}$ denote the sets of impassable and passable edges maintained by the server, respectively. Each device $n \in \mathcal{N}$ shares the information on impassable and passable edges directly with the server at each GPS positioning interval I_{GPS} if the communication infrastructure (e.g., a cellular network and/or a wireless LAN) still remains. When the communication infrastructure is (temporarily) unavailable due to a disaster and the communication with the server cannot be established, the scheme utilizes a DTN, which enables the end-to-end communications through the store-carry-forward paradigm by repeatedly conducting the D2D communications. The method of sharing information between devices is the same as that between the device and the server. **In this paper, to focus on the potential capability of automatic evacuation guiding, we simply assume that each device and server can fully synchronize their information on impassable and passable edges during their contact period. In future work, we will consider the limitation of information sharing due to the wireless communication overhead.**

In this paper, we adopt the risk-aware route selection algorithm proposed in the previous work [5]. In this algorithm, to achieve both speedy and safe evacuation, the device $n \in \mathcal{N}$ first enumerates the K shortest routes from the current location to the nearest refuge, and then selects the route with the maximum reachability, which is derived from the road blockage probability, from the enumerated ones. Note that it considers the road blockage probability p_e to be 1 (resp. 0) for each edge $e \in \hat{\mathcal{E}}_n^{\text{block}}$ ($e \in \hat{\mathcal{E}}_n^{\text{pass}}$). Please refer to [5] for the detail of the route calculation algorithm.

4. Impact of the presence of outliers taking unexpected evacuation movement

This section analyzes how the presence of outliers taking unexpected evacuation movement affects the **existing** automatic evacuation guiding scheme. First, Section 4.1 describes **some extensions** of the **existing** scheme to cope with the unexpected evacuation movement. Next, we investigate the impact of unexpected evacuation movement on the scheme **through simulations** in Section 4.2.

4.1. *Required extensions of the existing scheme*

In this section, we show that the automatic evacuation guiding scheme described in Section 3 needs some extensions when part of the evacuees are outliers taking unexpected evacuation movement. The information

on edges estimated as passable is always correct regardless of the type of evacuees (i.e., normal ones or outliers) under the assumption that the GPS positioning error can be ignored. On the other hand, as for the information on edges estimated as impassable, the estimation by devices of normal evacuees is always correct while that by devices of outliers can be either correct or incorrect.

The above discussion indicates that the estimation results may differ among devices even for the same edge in the presence of outliers. Therefore, in the **existing** scheme described in Section 3, we extend the information management at each device as follows. If a device $n \in \mathcal{N}$ estimates that an edge $e \in \mathcal{E}$ is impassable (resp. passable), it adds this information as an *impassable pair* (resp. *passable pair*) (e, n) to its own set $\hat{\mathcal{S}}_n^{\text{block}}$ (resp. $\hat{\mathcal{S}}_n^{\text{pass}}$) of impassable pairs (resp. passable pairs). The device n shares $\hat{\mathcal{S}}_n^{\text{block}}$ and $\hat{\mathcal{S}}_n^{\text{pass}}$ with other devices and the server as in the original scheme. For convenience, we denote the sets of impassable and passable pairs maintained by the server by $\hat{\mathcal{S}}_{\text{server}}^{\text{block}}$ and $\hat{\mathcal{S}}_{\text{server}}^{\text{pass}}$, respectively.

As a result, a device $n \in \mathcal{N}$ may have both an impassable pair $(e, m) \in \hat{\mathcal{S}}_n^{\text{block}}$ and a passable pair $(e, m') \in \hat{\mathcal{S}}_n^{\text{pass}}$ ($m, m' \in \mathcal{N}$) for some edge $e \in \mathcal{E}$. Here, the estimation result for a passable edge is always correct as mentioned above. **If** both an impassable pair $(e, m) \in \hat{\mathcal{S}}_n^{\text{block}}$ and a passable pair $(e, m') \in \hat{\mathcal{S}}_n^{\text{pass}}$ exist for an edge $e \in \mathcal{E}$, the passable pair is preferentially used. That is, the device n updates the set $\hat{\mathcal{E}}_n^{\text{block}}$ (resp. $\hat{\mathcal{E}}_n^{\text{pass}}$) of edges that the device n recognizes as impassable (resp. passable) edges by the following operations: $\hat{\mathcal{E}}_n^{\text{pass}} \leftarrow \{e \in \mathcal{E} \mid (e, m) \in \hat{\mathcal{S}}_n^{\text{pass}}, m \in \mathcal{N}\}$ and $\hat{\mathcal{E}}_n^{\text{block}} \leftarrow \{e \in \mathcal{E} \mid (e, m) \in \hat{\mathcal{S}}_n^{\text{block}}, m \in \mathcal{N}\} \setminus \hat{\mathcal{E}}_n^{\text{pass}}$. As in the original automatic evacuation guiding scheme, the application of the device n sets the road blockage probability p_e to be 1 (resp. 0) for each edge $e \in \hat{\mathcal{E}}_n^{\text{block}}$ (resp. $e \in \hat{\mathcal{E}}_n^{\text{pass}}$).

4.2. Simulation for evaluating the impact of the presence of outliers

4.2.1. Simulation model

We use the same simulation settings used in the previous work [5]. We use the automatic evacuation guiding simulator, which is developed by extending the ONE simulator [26]. As the target region, we use a 2,600 m \times 1,700 m road map of the Arako school district in Nagoya City, Japan (Figure 4). The graph $G = (\mathcal{V}, \mathcal{E}, f, g)$ of the region has 939 vertices and 1,510 edges, and there are five refuges within the region (blue squares). Each edge $e \in \mathcal{E}$ of the graph is associated with the road blockage probability p_e [22]. We assume that a disaster occurs immediately after the start of the simulation and each edge $e \in \mathcal{E}$ becomes blocked with the road blockage probability p_e . The set of blocked edges is denoted by $\mathcal{E}^{\text{block}}$. In the following, we assume that the state of each edge does not change during the simulation. More realistically, new impassable edges may arise due to aftershocks and/or impassable edges may change to passable with the help of restoration. These more complicated situations are left for future work.

There are N^{normal} normal evacuees and N^{outlier} outliers in the road network. Let $\mathcal{N}^{\text{normal}} \subset \mathcal{N}$ and $\mathcal{N}^{\text{outlier}} \subset \mathcal{N}$ denote the sets of devices owned by the normal evacuees and the outliers, respectively. ($\mathcal{N} = \mathcal{N}^{\text{normal}} \cup \mathcal{N}^{\text{outlier}}$.) At the start of the simulation ($t = 0$), each evacuee (normal or outlier) is initially

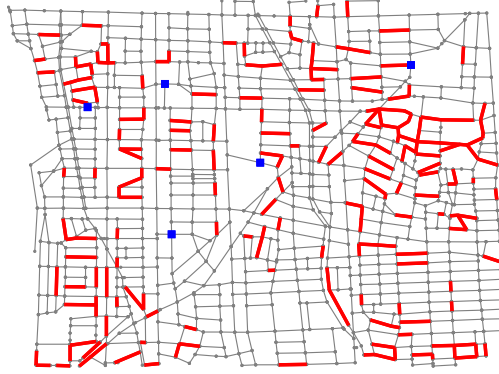


Figure 4: Road map of the Arako school district in Nagoya City. The **thick red** lines indicate (examples of) impassable edges, and the blue squares indicate refuges.

located at a vertex s chosen uniformly from \mathcal{V} . **At the same time**, the application is launched at the device owned by the evacuee **and recommends a route to the nearest refuge based on the risk-aware route selection scheme [5]**. We set the GPS positioning interval $I_{\text{GPS}} = 5$ s. Each evacuee starts moving at a random time in $[0, 200]$ with a travel speed of 4 km/h. Each normal evacuee will move to the nearest refuge along with the recommended route while each outlier behaves as follows. The outlier with the device n uniformly chooses a vertex v ($s \neq v$) from \mathcal{V} as his/her destination and takes the *shortest-path-movement* from the current location s to the destination v . In the shortest-path-movement, the outlier follows the shortest path from the current location to the destination v without using the information on impassable and passable edges estimated by the device. If the outlier encounters a blocked edge $e_h \in \mathcal{E}^{\text{block}}$ on the calculated shortest path $(s, e_1, v_1, e_2, v_2, \dots, v_{h-1}, e_h, v_h, \dots, v)$, he/she memorizes e_h as blocked and updates his/her own memory $\hat{\mathcal{E}}_{\text{evac},n}^{\text{block}}$, i.e., the set of impassable edges recognized by himself/herself. Note that $\hat{\mathcal{E}}_{\text{evac},n}^{\text{block}}$ is not necessarily equal to the device n 's estimation, i.e., $\mathcal{E}_n^{\text{block}}$. The outlier then finds the shortest path from the current location v_{h-1} to the destination v on $G = (\mathcal{V}, \mathcal{E} \setminus \hat{\mathcal{E}}_{\text{evac},n}^{\text{block}}, f, g)$ and proceeds along the path. If the outlier arrives at the destination v or there is no path to v , he/she stops the movement. The simulation time is set to $T_{\text{max}} = 3600$ s. In all the simulations, we confirmed that each evacuee arrived at his/her destination or failed to find a route there before T_{max} .

In this simulation, we basically assume a scenario called *no-communication-infrastructure scenario* where the communication infrastructure is unavailable due to the disaster. In this case, $\hat{\mathcal{S}}_{\text{server}}^{\text{block}}$ and $\hat{\mathcal{S}}_{\text{server}}^{\text{pass}}$ are always empty, and the information is shared among devices only through D2D communications. In the following experiments, we refer to the no-communication-infrastructure scenario with $N^{\text{normal}} = 200$ as the *base case*, which will be used as the default experimental condition unless otherwise noted. For comparison, in some experiments, we also consider another scenario called *with-communication-infrastructure scenario* in which all the devices can communicate with the server via the communication infrastructure. We set the

transmission range to be 10 m.

As for the comparison schemes, we evaluate the ideal evacuation movement (called *ideal*), in which all the normal evacuees know all impassable edges before the start of evacuation, and the legacy evacuation movement (called *no-system*), in which all the normal evacuees and outliers take the shortest-path-movement without using the automatic evacuation guiding scheme (that is, do not share impassable and passable pairs).

The average time to complete evacuation and the success ratio of evacuation guiding for normal evacuees are used as evaluation measures of evacuation movement. Here, the failure of evacuation guiding for a normal evacuee is defined as a situation in which the application of the device owned by the evacuee cannot find a route to any refuge using the information on edges estimated as impassable. The *success ratio of evacuation guiding* is defined as the ratio of the number of normal evacuees who reach refuges to the total number of normal evacuees. The *evacuation completion time* is defined as the time required for a normal evacuee to reach a refuge from the start of the evacuation, and the average evacuation completion time is defined as the average time among the normal evacuees who reach refuges.

For each simulation, the initial location of each evacuee, the destination of each outlier, and the start time of the movement of each evacuee are randomly determined while the state of each edge $e \in \mathcal{E}$ is determined with the road blockage probability p_e . In what follows, we show the averages of 50 simulations. We confirmed that about 13% of the whole edges were set to be impassable in average.

4.2.2. *Simulation results of the success ratio of evacuation guiding and average evacuation completion time for normal evacuees in the presence of outliers*

First, we evaluate the negative impact of the presence of outliers on the evacuation movement of normal evacuees. In this simulation, the number of outliers, N^{outlier} , is varied up to twice the number of normal evacuees, N^{normal} (i.e., $0 \leq N^{\text{outlier}} \leq 2N^{\text{normal}}$). Specifically, we set $N^{\text{normal}} = 200$ and change N^{outlier} from 0 to 400 in 100 increments. We will also show the larger-scale simulation experiments with over 1,000 evacuees in Section 5.2.2.

Figures 5 and 6 show the impact of the number N^{outlier} of outliers on the success ratio of evacuation guiding and average evacuation completion time, respectively. The 95% confidence intervals are also shown. First, we focus on the success ratio of evacuation guiding. In the with-communication-infrastructure scenario, the success ratios are 97.3%, 96.9%, 96.3% in the cases of $N^{\text{outlier}} = 0, 200, 400$, respectively, while in the no-communication-infrastructure scenario, the success ratios are 97.3%, 96.8%, 96.2% in the cases of $N^{\text{outlier}} = 0, 200, 400$, respectively. This indicates that the deterioration of the success ratio of evacuation guiding is limited in response to the increase in N^{outlier} . In other words, the concern about the evacuation failure due to the misestimation of passable edges as impassable by outliers (e.g., Figure 2 in Section 1) would not be a critical issue. (We will further discuss this phenomenon later.) We also confirm that the presence or absence of existing communication infrastructure has a negligible effect because of D2D communications. **The main**

reasons can be explained as follows. At first, in case of evacuation guiding, trajectories of evacuees moving to the same refuge tend to be similar. This will increase the opportunities of direct communications with others and their devices are expected to have the road-state estimation of surrounding road segments. This tendency is accelerated with increase of evacuees.

Next, we focus on the average evacuation completion time. The average evacuation completion time of ideal (resp. no-system) exhibits 558.1s (resp. 776.0s), which can be regarded as the lower (resp. upper) bound. The average evacuation completion time monotonically worsens with N^{outlier} regardless of the presence or absence of communication infrastructure. In particular, we observe that the average evacuation completion time increases by 76.4s (resp. 55.6s) in case of no-communication-infrastructure (resp. with-communication-infrastructure) by comparing the results of $N^{\text{outlier}} = 200$ with those of $N^{\text{outlier}} = 0$. These increases cannot be negligible compared with the introduction effects of the automatic evacuation guiding scheme (i.e., the difference of the average evacuation completion time between with and without the scheme), which become 139.9s (with-communication-infrastructure scenario) and 159.5s (no-communication-infrastructure scenario) when there are no outliers ($N^{\text{outlier}} = 0$), respectively. These results indicate that the information on edges misestimated as impassable by outliers would worsen the average evacuation completion time by causing unnecessary detours.

Finally, we focus on the impact of the presence or absence of communication infrastructure. The average evacuation completion time in the no-communication-infrastructure scenario is worse than that in the with-communication-infrastructure scenario in case of $N^{\text{outlier}} < 200$ while there is almost no difference between them in case of $N^{\text{outlier}} \geq 200$. This is because the edge state information is actively shared through D2D communications even without the communication infrastructure if a sufficiently large number of outliers exist. In the following analysis, considering the fact that the trends of the results were similar regardless of the presence or absence of communication infrastructure, we only present the results of the no-communication-infrastructure scenario, unless otherwise stated.

4.2.3. *Simulation results of the impact of impassable and passable pairs shared by outliers*

In this subsection, we analyze how impassable and passable pairs shared by outliers affect the success ratio of evacuation guiding and the average evacuation completion time. In general, we can expect that the increase of outliers will cause a larger number of edges misestimated as impassable, which may deteriorate the success ratio of evacuation guiding. The above-mentioned results in Figure 5, however, are contrary to this expectation. To deeply analyze this phenomenon, we conduct additional simulations by considering the following four combinations depending on the presence/absence of sharing passable and impassable pairs by outliers.

- (i) The outliers share neither impassable nor passable pairs (*neither-impassable-nor-passable*).

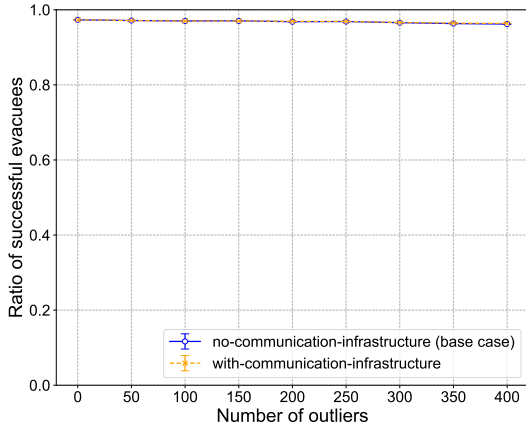


Figure 5: Relationship between the number of outliers and the success ratio of evacuation guiding in the **two scenarios**.

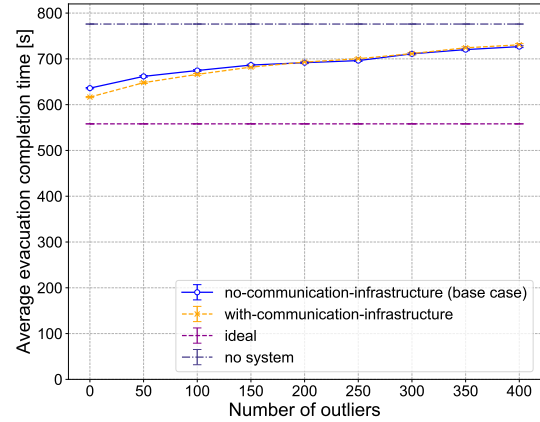


Figure 6: Relationship between the number of outliers and the average evacuation completion time of normal evacuees in the four scenarios.

- (ii) The outliers do not share passable pairs but share impassable ones (*impassable-only*).
- (iii) The outliers share passable pairs but do not share impassable ones (*passable-only*).
- (iv) The outliers share both passable and impassable pairs (*both-impassable-and-passable*).

The extended version of the automatic evacuation guiding scheme described in Section 4.1 corresponds to the both-impassable-and-passable. Note that realizing the other three methods in a real environment is a challenging issue because a new mechanism is required for the application to estimate the type of each evacuee (normal or outlier), as discussed in Section 1.

Figures 7 and 8 show the effects of the information shared by outliers on the success ratio of evacuation guiding and average evacuation completion time, respectively, when N^{outlier} is varied from 0 to 400 in 100 increments. Focusing on Figure 7, we first confirm that the impassable-only significantly deteriorates the success ratio of evacuation guiding with N^{outlier} , compared with the other three methods. The remaining three methods maintain relatively high success ratios regardless of N^{outlier} . This result indicates the following: Although impassable pairs misestimated by outliers may cause the evacuation guiding failure, at the same time, it can be mitigated by the increase of passable pairs shared by outliers.

Next, focusing on Figure 8, we confirm that the average evacuation completion time of the impassable-only reaches the peak at $N^{\text{outlier}} = 200$ and decreases in $N^{\text{outlier}} > 200$. Note that the latter decrease accompanies the deterioration of the success ratio of evacuation guiding (of normal evacuees). Compared to the impassable-only, the both-impassable-and-passable suppresses the deterioration of the average evacuation completion time in $N^{\text{outlier}} \leq 200$ thanks to passable pairs estimated by outliers, but the average evacuation

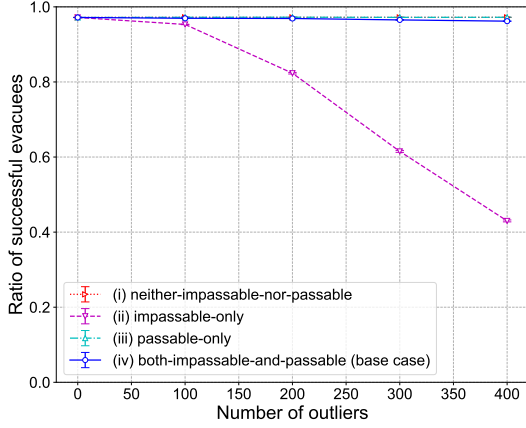


Figure 7: Relationship between the number of outliers and the success ratio of evacuation guiding when the outliers share or do not share passable and impassable pairs.

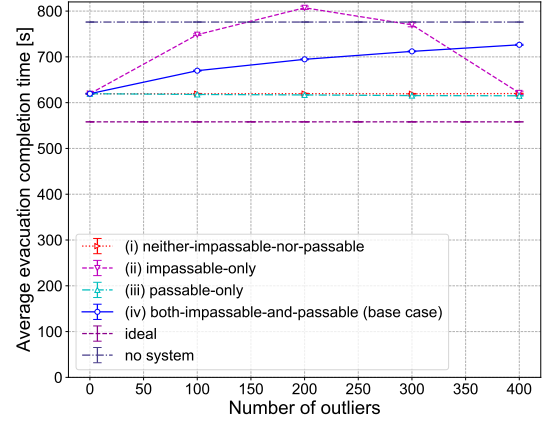


Figure 8: Relationship between the number of outliers and the average evacuation completion time of normal evacuees when the outliers share or do not share passable and impassable pairs.

completion time of the both-impassable-and-passable is worse than the other two methods in $N^{\text{outlier}} \leq 200$. As mentioned above, it should be noted that a mechanism for estimating the type of each evacuee (normal or outlier) is required to realize the methods other than the both-impassable-and-passable.

The above results indicate that there is room for improvement in the both-impassable-and-passable (i.e., the extended version of the automatic evacuation guiding scheme in Section 4.1) from the viewpoint of the average evacuation completion time.

4.2.4. Simulation results of the transition of shared status of passable and impassable pairs

In this subsection, we focus on the transition of the estimated information (passable or impassable) of each actually passable edge $e \in \mathcal{E}^{\text{pass}}$, where the misestimation of passable edges as impassable may have a negative impact on the evacuation movement of normal evacuees. A device $n \in \mathcal{N}$ can have one of the following five *estimated states* for each actually passable edge $e \in \mathcal{E}^{\text{pass}}$. Let $n' \in \mathcal{N}^{\text{outlier}}$ and $n'' \in \mathcal{N}$.

- Unknown state where no information is received (i.e., *no-passable-no-blocked (NPNB)*).
- Only a passable pair $(e, n'') \in \hat{\mathcal{S}}_n^{\text{pass}}$ is received (i.e., *first-passable-no-blocked (FPNB)*).
- An impassable pair $(e, n') \in \hat{\mathcal{S}}_n^{\text{block}}$ is received after a passable pair $(e, n'') \in \hat{\mathcal{S}}_n^{\text{pass}}$ is received (i.e., *first-passable-later-blocked (FPLB)*).
- Only an impassable pair $(e, n') \in \hat{\mathcal{S}}_n^{\text{block}}$ is received (i.e., *first-blocked-no-passable (FBNP)*).

- (e) A passable pair $(e, n'') \in \hat{\mathcal{S}}_n^{\text{pass}}$ is received after an impassable pair $(e, n') \in \hat{\mathcal{S}}_n^{\text{block}}$ is received (i.e., *first-blocked-later-passable (FBLP)*).

The estimated state of an edge $e \in \mathcal{E}^{\text{pass}}$ may change over time. The estimated state of each edge $e \in \mathcal{E}^{\text{pass}}$ is initially set to be NPNB, and then it transitions to FPNB (resp. FBPN) if the device n receives a passable (resp. an impassable) pair corresponding to the edge e from other evacuees. When the device n receives an impassable pair (e, n') (resp. a passable pair (e, n'')) for the edge e with the estimated state FPNB (resp. FBPN) from the device $n' \in \mathcal{N}^{\text{outlier}}$ of an outlier (resp. device $n'' \in \mathcal{N}$ of a normal evacuee), the estimated state of the edge e transitions to FPLB (resp. FBLP). After that, no further transition occurs. As described in Section 4.1, when the device n has both a passable pair $(e, n') \in \hat{\mathcal{S}}_n^{\text{block}}$ ($n' \in \mathcal{N}^{\text{outlier}}$) and an impassable pair $(e, n'') \in \hat{\mathcal{S}}_n^{\text{pass}}$ ($n'' \in \mathcal{N}$) for an edge e , it estimates e as passable, i.e., $e \in \hat{\mathcal{E}}_n^{\text{pass}}$. As a result, the device $n \in \mathcal{N}^{\text{normal}}$ of the normal evacuee can correctly estimate the edge e with the estimated state either FPNB or FPLB as passable, and thus there is no negative impact on the normal evacuees. On the other hand, the state FBLP of the edge e may negatively affect the evacuation movement of the normal evacuees. It should be noted that the edge with the estimated state FBLP can correctly be estimated as passable but the state FBPN is always passed through before reaching the estimated state FBLP.

We clarify how the number of edges with either of the above five estimated states changes over time for actually passable edges $e \in \mathcal{E}^{\text{pass}}$. Since the five estimated states are exclusive with each other and we assume that $\mathcal{E}^{\text{pass}}$ does not change, we focus on the four estimated states except for the estimated state NPNB. In addition, to investigate the effect on the evacuation movement of normal evacuees, we focus on the set $\mathcal{E}_{\text{evac}}^{\text{pass}}$ of actually passable edges that have been included in the recommended routes of the normal evacuees. In this simulation, we observed that the average of $|\mathcal{E}_{\text{evac}}^{\text{pass}}|$ was 722. For simplicity of evaluation, we use the with-communication-infrastructure scenario where all passable and impassable pairs estimated by each device are collected to the server and shared immediately with all devices.

We define the set of edges with either of the above four estimated states (i.e., FPNB, FPLB, FBPN, and FBLP) recognized by the server at a certain time t as follows:

$$\begin{aligned}\hat{\mathcal{E}}_{\text{server}}^{\text{FPNB}}(t) &= \{e \in \mathcal{E}_{\text{evac}}^{\text{pass}} \mid \min_{m \in \mathcal{N}} T_{\text{server}}^{\text{pass}}(e, m) \leq t, \min_{m' \in \mathcal{N}^{\text{outlier}}} T_{\text{server}}^{\text{block}}(e, m') > t\}, \\ \hat{\mathcal{E}}_{\text{server}}^{\text{FPLB}}(t) &= \{e \in \mathcal{E}_{\text{evac}}^{\text{pass}} \mid \min_{m \in \mathcal{N}} T_{\text{server}}^{\text{pass}}(e, m) < \min_{m' \in \mathcal{N}^{\text{outlier}}} T_{\text{server}}^{\text{block}}(e, m') \leq t\}, \\ \hat{\mathcal{E}}_{\text{server}}^{\text{FBPN}}(t) &= \{e \in \mathcal{E}_{\text{evac}}^{\text{pass}} \mid \min_{m' \in \mathcal{N}^{\text{outlier}}} T_{\text{server}}^{\text{block}}(e, m') \leq t, \min_{m \in \mathcal{N}} T_{\text{server}}^{\text{pass}}(e, m) > t\}, \\ \hat{\mathcal{E}}_{\text{server}}^{\text{FBLP}}(t) &= \{e \in \mathcal{E}_{\text{evac}}^{\text{pass}} \mid \min_{m' \in \mathcal{N}^{\text{outlier}}} T_{\text{server}}^{\text{block}}(e, m') \leq \min_{m \in \mathcal{N}} T_{\text{server}}^{\text{pass}}(e, m) \leq t\},\end{aligned}$$

where $T_{\text{server}}^{\text{pass}}(e, m)$ (resp. $T_{\text{server}}^{\text{block}}(e, m')$) denotes the first time when a passable pair (e, m) (resp. an impassable pair (e, m')) estimated by a device $m \in \mathcal{N}$ (resp. $m' \in \mathcal{N}^{\text{outlier}}$ of an outlier) is recorded on the server (the value is ∞ if it is not recorded on the server).

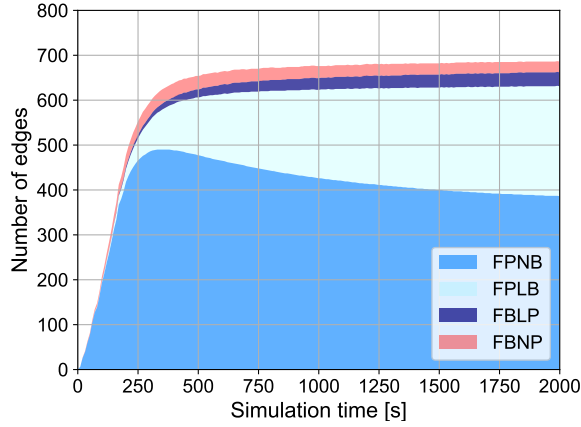


Figure 9: Transition of $|\hat{\mathcal{E}}_{\text{server}}^{\text{FPNB}}(t)|$, $|\hat{\mathcal{E}}_{\text{server}}^{\text{FPLB}}(t)|$, $|\hat{\mathcal{E}}_{\text{server}}^{\text{FBLP}}(t)|$, and $|\hat{\mathcal{E}}_{\text{server}}^{\text{FBNP}}(t)|$.

In what follows, we assume $N^{\text{normal}} = 200$ and $N^{\text{outlier}} = 100$. Note that we also confirmed the same trend in other cases, i.e., $N^{\text{outlier}} = 200, 300$. Figure 9 shows the transition of $|\hat{\mathcal{E}}_{\text{server}}^{\text{FPNB}}(t)|$, $|\hat{\mathcal{E}}_{\text{server}}^{\text{FPLB}}(t)|$, $|\hat{\mathcal{E}}_{\text{server}}^{\text{FBLP}}(t)|$, and $|\hat{\mathcal{E}}_{\text{server}}^{\text{FBNP}}(t)|$. $\hat{\mathcal{E}}_{\text{server}}^{\text{FPNB}}(t)$, $\hat{\mathcal{E}}_{\text{server}}^{\text{FPLB}}(t)$, and $\hat{\mathcal{E}}_{\text{server}}^{\text{FBLP}}(t)$ are drawn in bluish colors, while $\hat{\mathcal{E}}_{\text{server}}^{\text{FBNP}}(t)$ is drawn in a reddish color. From this figure, we observe that the number of edges estimated as passable (i.e., $|\hat{\mathcal{E}}_{\text{server}}^{\text{FPNB}}(t) \cup \hat{\mathcal{E}}_{\text{server}}^{\text{FPLB}}(t) \cup \hat{\mathcal{E}}_{\text{server}}^{\text{FBLP}}(t)|$) steeply increases at the initial phase, and then almost converges at the average evacuation completion time $t = 674.6$ s. On the other hand, the number of edges that are still misestimated as impassable (i.e., $|\hat{\mathcal{E}}_{\text{server}}^{\text{FPNB}}(t)|$) also increases at the initial phase. In $t \geq 300$, we can also confirm how part of $\hat{\mathcal{E}}_{\text{server}}^{\text{FPNB}}(t)$ (resp. $\hat{\mathcal{E}}_{\text{server}}^{\text{FBNP}}(t)$) transitions to $\hat{\mathcal{E}}_{\text{server}}^{\text{FPLB}}(t)$ (resp. $\hat{\mathcal{E}}_{\text{server}}^{\text{FBLP}}(t)$). Specifically, we confirm that $|\hat{\mathcal{E}}_{\text{server}}^{\text{FPNB}}(t)|$ is larger than $|\hat{\mathcal{E}}_{\text{server}}^{\text{FBNP}}(t)|$. However, there are some edges remaining in $\hat{\mathcal{E}}_{\text{server}}^{\text{FBNP}}(t)$ until the end of the simulation. Although the number of these edges (i.e., 33) is limited compared to the total number of target edges, i.e., $|\mathcal{E}_{\text{evac}}^{\text{pass}}| = 722.0$, they could worsen the evacuation time of normal evacuees as shown in Section 4.2.2.

Since the devices owned by outliers correctly estimate passable edges, it may improve the evacuation movement of normal evacuees. We analyzed the proportion of edges estimated to be passable first by normal evacuees or outliers. We omit the results due to the space limitation, but we confirmed that normal evacuees and outliers find almost the same number of passable edges per person and most of them are found before the average evacuation completion time. These results suggest that the information on edges estimated as passable by outliers contributes to the improvement of the evacuation movement of normal evacuees.

4.2.5. *Simulation results of the impact of the presence of outliers on the evacuation completion time for each normal evacuee*

In this subsection, we consider how the presence of outliers affects the evacuation completion time for each normal evacuee. For this purpose, we run the following two simulations. In the first simulation, we

consider that there are no outliers ($N^{\text{outlier}} = 0$) and $N^{\text{normal}} = 200$ normal evacuees, who are randomly placed at vertices on the map G , and measure the evacuation completion time τ_n of each normal evacuee who owns the device $n \in \mathcal{N}^{\text{normal}}$. In the second simulation, we keep $N^{\text{normal}} = 200$ normal evacuees with their initial locations in the first simulation and newly add $N^{\text{outlier}} = 100$ outliers randomly placed at vertices on the map G . In the second simulation, we also measure the evacuation completion time τ'_n of each normal evacuee with the device $n \in \mathcal{N}^{\text{normal}}$. **Let Δ_n be the difference, i.e., $\tau'_n - \tau_n$, of the evacuation completion time between the two simulations, where $\Delta_n > 0$ (resp. $\Delta_n < 0$) means the deterioration (resp. improvement) of evacuation completion time of the normal evacuee with the device n . If the presence of outliers causes the evacuation guiding failure (resp. success) of normal evacuee with the device n , we regard Δ_n as the maximum (resp. minimum) difference of evacuation completion time among all the normal evacuees with successful evacuation between the two simulations.**

We conduct the 50 independent simulations and show the average of their results. Figure 10 illustrates the distribution of Δ_n where the normal evacuees are sorted in ascending order of Δ_n . Note that we show two kinds of results: One is the result for the base case ($M = 1$) and another one ($M = 2$) will be explained in Section 5.2. From the figure, we observe that the 26.5% of normal evacuees degrade the evacuation completion time by more than 100s due to the presence of outliers, which is caused by a small number of impassable pairs misestimated by outliers according to the discussion in Section 4.2.4. On the other hand, we also observe that the 7.5% of them improve the evacuation completion time by more than 100s.

The left (resp. right) side in Figure 11 depicts an example of the evacuation movement whose evacuation completion time worsens by an impassable pair. Here, in case of $N^{\text{outlier}} = 0$, the normal evacuee located at the green point succeeds in evacuating to the blue square refuge along the blue solid path. On the other hand, in case of $N^{\text{outlier}} = 100$, the same normal evacuee is forced to take the longer detour (i.e., green dotted path), due to the information on the passable edge B misestimated as impassable by an outlier. As a result, we confirm that the evacuation completion time of this evacuee becomes 377.4s in case of $N^{\text{outlier}} = 0$ while it becomes 550.5s in case of $N^{\text{outlier}} = 100$ (i.e., the deterioration of the evacuation completion time becomes 176.1s) due to one misestimated impassable pair. The right side in Figure 11 shows an example of the evacuation movement whose evacuation completion time improves by an impassable pair. As in the first case, the normal evacuee located at the green point takes the blue solid (resp. green dotted) path in case of $N^{\text{outlier}} = 0$ (resp. $N^{\text{outlier}} = 100$). In this case, the evacuation completion time of $N^{\text{outlier}} = 100$ improves by 254.9s compared with that of $N^{\text{outlier}} = 0$, with the help of an impassable pair of the edge B, which is correctly estimated by an outlier.

These results indicate that the presence of outliers causes both the increase and decrease in the evacuation completion time of normal evacuees, but many of them lead to the deterioration of the evacuation completion time.

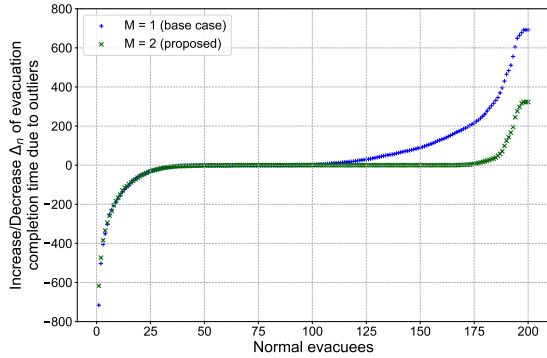


Figure 10: Distribution of increase/decrease Δ_n of evacuation completion time due to outliers.

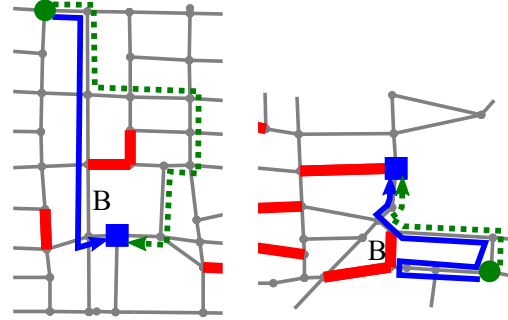


Figure 11: Examples that the presence of outliers deteriorates (left) and improves (right) the evacuation completion time of normal evacuees.

5. Road-state estimation method robust against unexpected evacuation movement

5.1. Proposed method

In the extended version of the automatic evacuation guiding scheme described in Section 4.1, the device of a normal evacuee wrongly recognizes a passable edge as impassable if it only has impassable pair(s) of the corresponding edge. This misunderstanding would be corrected by further retrieval of a correct passable pair, but we have confirmed that a small number of these passable edges misestimated as impassable have a non-negligible negative impact in terms of the average evacuation completion time of normal evacuees as shown in Section 4.2.2. Therefore, we need some countermeasure against such misestimation of passable edges as impassable. Ideally, the device owned by an outlier should stop the spread of misestimated information, but it requires for the device to detect the unexpected movement itself, which is not easy to solve. Moreover, if the communication infrastructure is not available and information sharing is realized by a DTN, it is not easy to remove misestimated information from the network once it has been spread. Therefore, in this section, we consider a method to mitigate the misestimation locally at devices owned by normal evacuees.

Specifically, considering the possibility that the estimated results by others may contain errors, the device $n \in \mathcal{N}$ delays to judge an edge e as impassable until it collects at least M ($M \geq 1$) impassable pairs of the edge e . Note that if the device n has its own impassable pair (e, n) for an edge e , it immediately and correctly judges e as impassable. As described in Section 4.1, if the device n has both impassable and passable pairs estimated by others for an edge e , it considers e to be passable.

As a result, the device n updates the set $\hat{\mathcal{E}}_n^{\text{block}}$ (resp. $\hat{\mathcal{E}}_n^{\text{pass}}$) of edges recognized by itself as impassable (resp. passable): $\hat{\mathcal{E}}_n^{\text{pass}} \leftarrow \{e \in \mathcal{E} \mid (e, m) \in \hat{\mathcal{S}}_n^{\text{pass}}, m \in \mathcal{N}\}$ and $\hat{\mathcal{E}}_n^{\text{block}} \leftarrow \{e \in \mathcal{E} \mid |\{m \mid (e, m) \in \hat{\mathcal{S}}_n^{\text{block}}, m \in \mathcal{N}, m \neq n\}| \geq M\} \cup \{e \in \mathcal{E} \mid (e, n) \in \hat{\mathcal{S}}_n^{\text{block}}\} \setminus \hat{\mathcal{E}}_n^{\text{pass}}$. The case of $M = 1$ is consistent with the extended version of the automatic evacuation guiding scheme described in Section 4.1. The increase of M improves

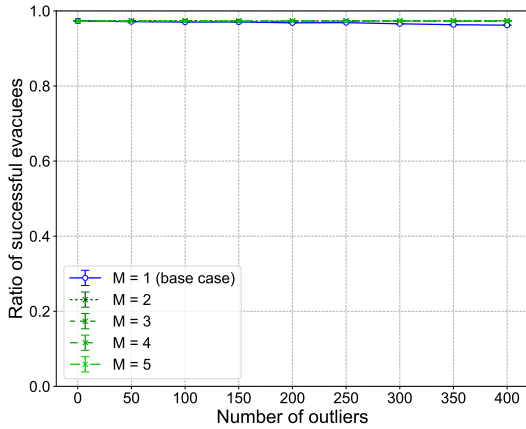


Figure 12: Relationship between the number of outliers and the success ratio of evacuation guiding as M varies.

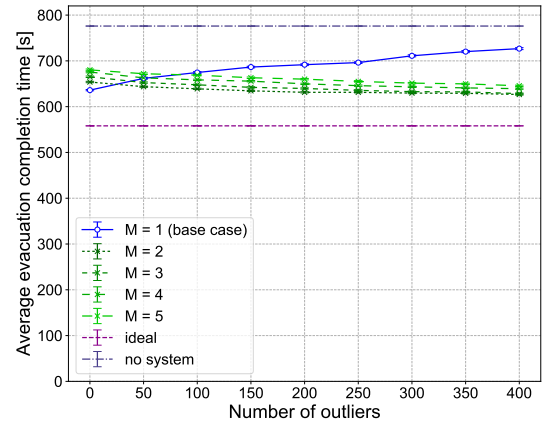


Figure 13: Relationship between the number of outliers and the average evacuation completion time as M varies.

the robustness of the method against the misestimation of passable edges as impassable while increasing the risk of encounters with actually impassable edges. To address this trade-off, we investigate an appropriate value of M in the next section.

5.2. Simulation results of the proposed method

In this subsection, we show the effectiveness of the proposed method through simulations. We do not conduct comparison with other methods because there are no attempts coping with the unexpected movement in any *automatic* evacuation guiding, to the best of our knowledge.

5.2.1. Trade-off between speediness and safety of evacuation

Figures 12 and 13 illustrate the success ratio of evacuation guiding and the average evacuation completion time in case of $M = 1, 2, \dots, 5$ when changing the number N^{outlier} of outliers from 0 to 400 in 50 increments. We first observe that the success ratio of evacuation guiding monotonically decreases with N^{outlier} , regardless of the value of M . Although the degree of decrease in the success ratio increases with the decrease of M , it is limited to about 1.0% even in case of $M = 1$.

Next, focusing on the average evacuation completion time, we confirm that it monotonically increases with N^{outlier} when $M = 1$ (note that we have already seen it in Section 4.2.2), which means that the increase in the number of passable edges misestimated as impassable by outliers hinders the evacuation of normal evacuees. On the other hand, in case of $M \geq 2$, we confirm that the average evacuation completion time monotonically decreases with the increase of N^{outlier} because the threshold M to regard an edge as impassable increases and the misestimation decreases. The increase in M , however, also increases the risk of encountering actually impassable edges, which will be evaluated later. Focusing on the no-outlier case

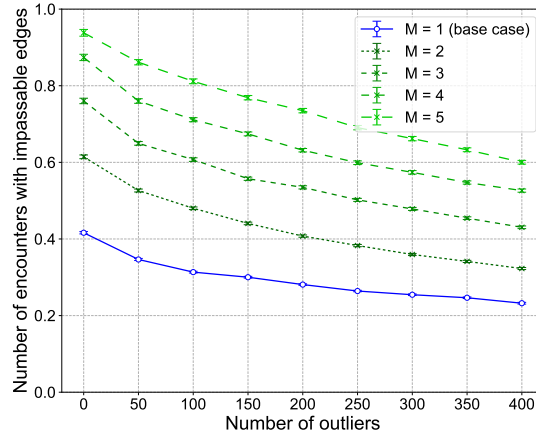


Figure 14: Relationship between the number of outliers in the base case and the number of encounters with impassable edges.

(i.e., $N^{\text{outlier}} = 0$), we observe that the average evacuation completion time increases as with M . This is because of the unnecessary delay in recognizing impassable edges in the case of $M \geq 2$, despite the correct estimation of impassable edges in the no-outlier case ($N^{\text{outlier}} = 0$). Note that we also confirm that the increase of the average evacuation completion time of $M = 2$ is limited to 2.8% compared with that of $M = 1$. In the range of $N^{\text{outlier}} \geq 50$, the average evacuation completion time of $M = 2$ is smaller than that of $M = 1$, whose improvements are 35.7s, 60.4s, and 100.1s when $N^{\text{outlier}} = 100, 200,$ and 400 , respectively. Furthermore, focusing on the increase or decrease in the evacuation completion time of individual normal evacuees in Figure 10, we confirm that the deterioration of the evacuation completion time of more than 100s is 9.5% when $M = 2$, which is significantly improved compared with the result of $M = 1$ (i.e., 26.5%).

Next, we evaluate the evacuation safety in terms of the number of encounters with impassable edges. Figure 14 depicts the average number of times that a normal evacuee encounters an impassable edge when the number N^{outlier} of outliers is varied from 0 to 400 in 50 increments. Focusing on $M = 1$ (i.e., the base case), we first observe that the risk of encountering an impassable edge monotonically decreases with N^{outlier} . This is because the normal evacuees more cautiously evacuate by sharing more impassable pairs, which may include misestimation, with the increase of N^{outlier} . It should be noted, however, that such evacuation movement leads to an increase in the average evacuation completion time, as shown in Figure 13. In addition, we can confirm that the increase of M tends to increase the risk of encountering an impassable edge, regardless of N^{outlier} . This is due to the fact that the recognition of impassable edges is delayed at normal evacuees due to the higher threshold M to detect impassable edges.

The above discussion shows that there is a trade-off between speediness (i.e., average evacuation completion time) and safety (i.e., risk of encountering impassable edges) of evacuation, which can be controlled by

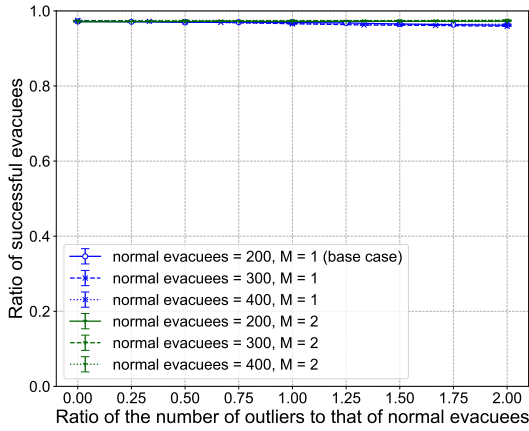


Figure 15: Success ratio of evacuation guiding relative to the ratio of normal evacuees to outliers.

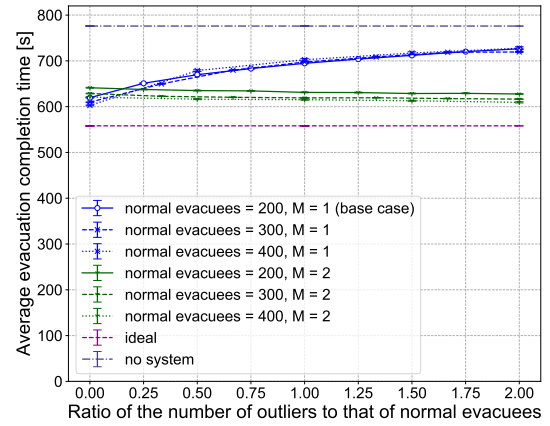


Figure 16: Average evacuation completion time relative to the ratio of normal evacuees to outliers.

M . To analyze the trade-off quantitatively, we simply adopt the linear evaluation function $f(x, y) = x + \alpha y$, where x is the deterioration (seconds) of the average evacuation completion time compared to the case of no outlier and $M = 1$, y is the number of times of encountering impassable road segments, and $\alpha \geq 0$ is a weighting parameter to control the preference on them. More specifically, α converts an encounter with a blocked road segment into the deterioration of evacuation completion time. We set $\alpha = 50$ and $\alpha = 100$. We omit the computation result of f due to the space limitation, but for all cases of N^{outlier} except for $N^{\text{outlier}} = 0$, setting $M = 2$ minimizes the value of f . Therefore, $M = 2$ can be an appropriate value that balances the speediness and safety of evacuation. Since the appropriate value of M may be affected by the number of evacuees, we will evaluate it in the next section.

For $M = 2, 3$, we conducted the same simulations on the transition of shared status of passable and impassable pairs as in Section 4.2.4. They are also omitted due to the space limitation, but we confirmed that the tendencies of $M = 2$ and $M = 3$ are almost the same as that of $M = 1$ except that the values of $|\hat{\mathcal{E}}_{\text{server}}^{\text{FBNP}}(t)|$ for $M = 2, 3$ are smaller than that for $M = 1$.

5.2.2. Impact of the number of evacuees

In this subsection, we evaluate the impact of the number of evacuees on the appropriate value of M . Figures 15 and 16 depict the success ratio of evacuation guiding and the average evacuation completion time in case of both $M = 1$ and $M = 2$ when varying the value of N^{outlier} from 0 to $2N^{\text{normal}}$ and $N^{\text{normal}}=200, 300, \text{ and } 400$, respectively. Note that the maximum number of evacuees is 1,200 ($N^{\text{normal}} = 400$ and $N^{\text{outlier}} = 800$) in the simulation. The results of $M = 1, 2$ when $N^{\text{normal}} = 200$ in Figures 15 and 16 correspond to those in Figures 12 and 13, respectively.

Focusing on $M = 1$, we first confirm that there is almost no effect of the number of evacuees on both

the success ratio of evacuation guiding and the average evacuation completion time even when increasing the value of N^{normal} from 200 to 300 or 400. Next, focusing on $M = 2$, we confirm that the increase of N^{normal} does not almost affect the success ratio of evacuation guiding but slightly deteriorates the average evacuation completion time. This is caused by the fact that the increase in the number of normal evacuees and outliers promotes the diffusion of passable pairs, which leads to the speedy understanding of passable edges as well as corrections of misestimated impassable pairs.

Let us discuss what value of M is appropriate. Although the results are omitted due to the space limitation, we confirm that if we set $\alpha = 100$, the evaluation function is minimized when $M = 2$ for $N^{\text{normal}} = 300, 400$ and all N^{outlier} except for $N^{\text{outlier}} = 0$. (In the cases of $N^{\text{outlier}} = 0$, $M = 1$ is the best because both the average evacuation completion time and the expected number of times of encountering impassable road segments deteriorate as M increases.) However, it is expected that if the number of outliers increases, the misestimations of passable road segments as impassable also increase, and thus there might be cases where $M \geq 3$ is more appropriate. Actually, if we set $\alpha = 50$, in some cases where $N^{\text{normal}} = 400$ and $N^{\text{outlier}} = 600, 800$, the optimal M changes from 2 to 3, but the value of the evaluation function for $M = 2$ is not much worse than that for $M = 3$. (For example, in the case of $N^{\text{normal}} = 400$ and $N^{\text{outlier}} = 800$, the value of f is 9.50 if $M = 2$ and 8.63 if $M = 3$.) Therefore, $M = 2$ can be appropriate for various situations.

6. Conclusion

In the existing automatic evacuation guiding scheme, some passable edges may be misestimated as impassable if part of evacuees behave as outliers taking unexpected movement, which differs from the movement expected by the scheme (i.e., moving to refuges). Such misestimation may have a negative impact on other normal evacuees by causing unnecessary detours. On the other hand, the presence of such outliers may also support the normal evacuation because the devices owned by outliers can correctly estimate and share passable edges.

In this paper, we have quantitatively analyzed these negative and positive impacts through simulation evaluations. As a result, we have found that the number of passable edges misestimated as impassable increases with the number of outliers but many of them can be corrected by the passable estimation given by devices of other outliers. We have also confirmed that the remaining passable edges misestimated as impassable are limited but they cause the increase of the average evacuation completion time of normal evacuees.

To address this problem, we have further improved the robustness of the automatic evacuation guiding scheme against such misestimation by delaying to judge an edge as impassable until a device collects at least M impassable pairs from others. Through the simulation results, we have shown that $M = 2$ achieves an appropriate balance between the speediness and safety in evacuation guiding, regardless of the number of

evacuees.

In future work, we plan to consider the applicability to temporal changes in edge states (i.e., appearance of new impassable edges due to aftershocks and/or transition from impassable to passable edges thanks to recovery work). We will also consider more complex behavior of outliers: combination of normal evacuation movement and unexpected one, partial use of information presented by their devices, and so on. **Theoretical investigation on the reason why setting $M \geq 2$ decreases the average evacuation completion time would be future work.**

References

- [1] Y. Iizuka, K. Yoshida, K. Iizuka, An effective disaster evacuation assist system utilized by an ad-hoc network, in: Proceedings of International Conference on Human-Computer Interaction, 2011, pp. 31–35. doi:10.1007/978-3-642-22095-1_7.
- [2] A. Fujihara, H. Miwa, Disaster evacuation guidance using opportunistic communication: The potential for opportunity-based service, Big Data and Internet of Things: A Roadmap for Smart Environments (2014) 425–446doi:10.1007/978-3-319-05029-4_18.
- [3] N. Komatsu, M. Sasabe, J. Kawahara, S. Kasahara, Automatic evacuation guiding scheme based on implicit interactions between evacuees and their mobile nodes, GeoInformatica 22 (1) (2018) 127–141. doi:10.1007/s10707-016-0270-1.
- [4] K. Fall, A delay-tolerant network architecture for challenged internets, in: Proceedings of the 2003 Conference on Applications, Technologies, Architectures, and Protocols for Computer Communications, 2003, pp. 27–34. doi:10.1145/863955.863960.
- [5] T. Hara, M. Sasabe, S. Kasahara, Geographical risk analysis based path selection for automatic, speedy, and reliable evacuation guiding using evacuees’ mobile devices, Journal of Ambient Intelligence and Humanized Computing 10 (6) (2019) 2291–2300. doi:10.1007/s12652-018-0826-z.
- [6] H. Nishiyama, M. Ito, N. Kato, Relay-by-smartphone: Realizing multihop device-to-device communications, IEEE Communications Magazine 52 (4) (2014) 56–65. doi:10.1109/MCOM.2014.6807947.
- [7] M. Otomo, K. Hashimoto, N. Uchida, Y. Shibata, Mobile cloud computing usage for onboard vehicle servers in collecting disaster data information, in: Proceedings of IEEE 8th International Conference on Awareness Science and Technology (iCAST), 2017, pp. 475–480. doi:10.1109/ICAwST.2017.8256504.
- [8] M. Misumi, T. Nishimura, N. Kamiyama, Placing information boxes to reduce power consumption in disaster communications using DTN, in: Proceedings of IEEE Global Communications Conference (GLOBECOM), 2021, pp. 1–6. doi:10.1109/GLOBECOM46510.2021.9685611.
- [9] Y. Kasai, M. Sasabe, S. Kasahara, Congestion-aware route selection in automatic evacuation guiding based on cooperation between evacuees and their mobile nodes, EURASIP Journal on Wireless Communications and Networking 2017 (164) (2017) 1–11. doi:10.1186/s13638-017-0948-6.
- [10] M. Misumi, N. Kamiyama, Evacuation-route recommendation using DTN with evacuee attributes in disasters, in: Proceedings of IEEE Wireless Communications and Networking Conference (WCNC), 2021, pp. 1–7. doi:10.1109/WCNC49053.2021.9417588.
- [11] F. Meng, G. Yuan, S. Lv, Z. Wang, S. Xia, An overview on trajectory outlier detection, Artificial Intelligence Review 52 (4) (2019) 2437–2456. doi:10.1007/s10462-018-9619-1.
- [12] J.-G. Lee, J. Han, X. Li, Trajectory outlier detection: A partition-and-detect framework, in: Proceedings of IEEE 24th International Conference on Data Engineering, 2008, pp. 140–149. doi:10.1109/ICDE.2008.4497422.

- [13] Z. Li, J. Han, M. Ji, L.-A. Tang, Y. Yu, B. Ding, J.-G. Lee, R. Kays, MoveMine: Mining moving object data for discovery of animal movement patterns, *ACM Transactions on Intelligent Systems and Technology* 2 (4) (2011) 1–32. doi:10.1145/1989734.1989741.
- [14] X. Li, Z. Li, J. Han, J.-G. Lee, Temporal outlier detection in vehicle traffic data, in: *Proceedings of IEEE 25th International Conference on Data Engineering*, 2009, pp. 1319–1322. doi:10.1109/ICDE.2009.230.
- [15] W. Kuang, S. An, H. Jiang, Detecting traffic anomalies in urban areas using taxi GPS data, *Mathematical Problems in Engineering* 2015 (2015) 1–14. doi:10.1155/2015/809582.
- [16] E. O. Eldawy, A. Hendawi, M. Abdalla, H. M. O. Mokhtar, FraudMove: Fraud drivers discovery using real-time trajectory outlier detection, *ISPRS International Journal of Geo-Information* 10 (11) (2021) 1–22. doi:10.3390/ijgi10110767.
- [17] M. X. Hoang, Y. Zheng, A. K. Singh, FCCF: Forecasting citywide crowd flows based on big data, in: *Proceedings of the 24th ACM International Conference on Advances in Geographic Information Systems (ACM SIGSPATIAL 2016)*, 2016, pp. 1–10. doi:10.1145/2996913.2996934.
- [18] E. M. Knorr, R. T. Ng, V. Tucakov, Distance-based outliers: Algorithms and applications, *The VLDB Journal* 8 (3) (2000) 237–253. doi:10.1007/s007780050006.
- [19] M. M. Breunig, H.-P. Kriegel, R. T. Ng, J. Sander, LOF: Identifying density-based local outliers, *ACM SIGMOD Record* 29 (2) (2000) 93–104. doi:10.1145/335191.335388.
- [20] J.-G. Lee, J. Han, K.-Y. Whang, Trajectory clustering: A partition-and-group framework, in: *Proceedings of the 2007 ACM SIGMOD International Conference on Management of Data*, Association for Computing Machinery, 2007, pp. 593–604. doi:10.1145/1247480.1247546.
- [21] X. Li, J. Han, S. Kim, H. Gonzalez, ROAM: Rule- and motif-based anomaly detection in massive moving object data sets, in: *Proceedings of the 2007 SIAM International Conference on Data Mining (SDM)*, Proceedings, Society for Industrial and Applied Mathematics, 2007, pp. 273–284. doi:10.1137/1.9781611972771.25.
- [22] City of Nagoya, Earthquake-resistance city development policy (in japanese), <http://www.city.nagoya.jp/jutakutoshi/cmsfiles/contents/0000002/2717/honpen.pdf>, Accessed 29 May 2022 (2015).
- [23] T. Hara, M. Sasabe, T. Matsuda, S. Kasahara, Capacitated refuge assignment for speedy and reliable evacuation, *ISPRS International Journal of Geo-Information* 9 (7) (2020) 442: 1–19. doi:10.3390/ijgi9070442.
- [24] M. A. Quddus, W. Y. Ochieng, L. Zhao, R. B. Noland, A general map matching algorithm for transport telematics applications, *GPS Solutions* 7 (3) (2003) 157–167. doi:10.1007/s10291-003-0069-z.
- [25] L. Zhu, J. R. Holden, J. D. Gonder, Trajectory segmentation map-matching approach for large-scale, high-resolution GPS data, *Transportation Research Record* 2645 (1) (2017) 67–75. doi:10.3141/2645-08.
- [26] A. Keränen, J. Ott, T. Kärkkäinen, The ONE simulator for DTN protocol evaluation, in: *Proceedings of the 2nd International Conference on Simulation Tools and Techniques*, 2009, pp. 1–10. doi:10.4108/ICST.SIMUTOOLS2009.5674.